

## 2.4 AE9 Templates Derived from CRRES Data

---

This section development of AE9  $K$ - $\Phi$  templates based on CRRES data. The AE9  $K$ - $\Phi$  templates are based on the CRRES MEA and HEEF data sets (Section 3.3.1). These data sets have been cross-calibrated and had data cleaning and corrections applied. The data sets span 440 days in 1990-1991, in particular covering very different states of the radiation belts before and after the March 1991 storm.

### 2.4.1 $K$ - $\Phi$ templates

#### 2.4.1.1 Processing of CRRES data

The strategy for creating AE9  $K$ - $\Phi$  templates was driven by the fact that the general shapes of electron energy spectra are highly variable. Investigation of this issue early in AE9 development identified that these energy spectra are typically exponential in the outer belt, power law outside the outer belt, and “bump-on-tail” in the slot region [Johnston *et al.*, 2013]. These bump-on-tail spectra, with a local minima (generally near  $\sim 0.6$  MeV) illustrate that a parametric fit scheme as used for protons was not feasible for electrons. Consequently it was determined to bin CRRES data in the standard  $K$ - $\Phi$  bins and use the resulting shapes to the extent possible, reverting to parametric fits where data was inadequate (i.e. near the limits of the  $K$ - $\Phi$ - $E$  space where CRRES data was lacking).

Data during solar proton events (SPEs) was removed, based on a NOAA-derived SPE list. Data was binned by standard AE9  $K$ - $\Phi$  bins and separated at day 82.0 of 1991 into pre-storm and post-storm. In each bin the following statistics were calculated for fluxes from each energy channel: mean, median, 25<sup>th</sup> percentile, 75<sup>th</sup> percentile, and 95<sup>th</sup> percentile. This produced five energy spectra in each bin. Bins with no data or very limited data were omitted.

To splice the MEA and HEEF data sets in energy coverage, MEA data was preferred over HEEF data if both were available (i.e. in the energy range 0.65-1.6 MeV). For each energy spectra in each bin, HEEF fluxes at energies  $\geq 1.6$  MeV were scaled so that the 1.6 MeV HEEF channel flux matched that of the 1.57 MeV MEA channel. Due to the contamination background and/or low counts in HEEF, the spectral tail at high energies was often flat or rising; channel fluxes for such tails at energies  $> 2$  MeV were omitted. Generally, HEEF data extended to higher energies at higher percentiles (where counts were above the noise/background); as available, the spectral shape at higher percentiles was scaled to fill missing high energy tails at lower percentiles.

These steps produced several spectral sets by  $K$ - $\Phi$  bin and by pre-/post-storm, at MEA/HEEF channel energies, forming the basis for subsequent steps individualized by template. Resulting energy spectra for several  $K$ - $\Phi$  bins are shown in Figure 20.

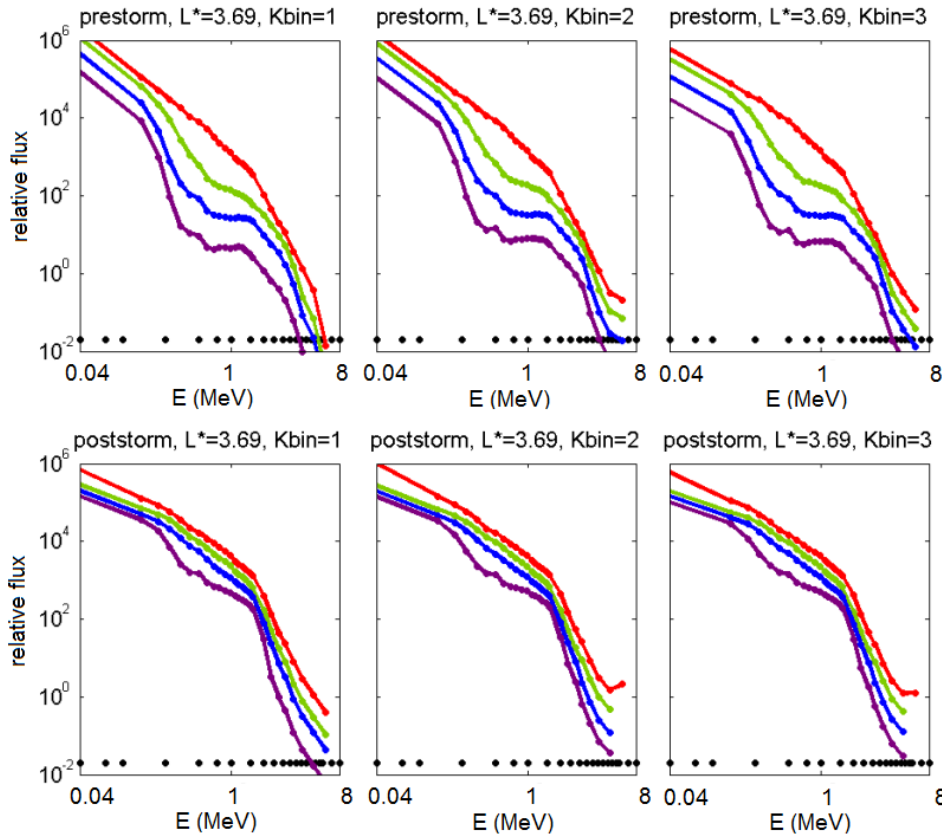


Figure 20. Illustrative flux vs. energy curves for various pre-templates, at  $L^* \sim 3.69$ . Spectra shown are 25<sup>th</sup> percentile (purple), median (blue), 75<sup>th</sup> percentile (green), and 95<sup>th</sup> percentile (red). Black dots indicate AE9 standard channel energies.

### 2.4.1.2 Production of base templates

The next step was to produce four basic templates from the above results, the four being pre-storm median and 95<sup>th</sup> percentile, and post-storm median and 95<sup>th</sup> percentile. The process discussed below basically applied these processes: interpolation and extrapolation of series of fluxes vs.  $K$ ,  $\Phi$ , or energy  $E$ ; filling missing bin/energies from nearest neighbors; and smoothing in  $K$ - $\Phi$  space. Such steps were applied to populate all  $K$ - $\Phi$  bins for CRRES channel energies, then the results were interpolated/extrapolated to populate the  $K$ - $\Phi$  bins for the standard AE9 energies.

Outline of steps for producing base templates:

- 1) Manual cleaning of flux vs.  $K$  for each energy and  $\Phi$  value (note: initial cleaning was done in  $K$  slices because of significant discontinuities in flux vs.  $K$  at constant  $\Phi$ , likely resulting from sampling issues in CRRES data). Figure 21 shows a sample slice in  $K$ .
- 2) Copying of spectral shape from 5.75 MeV to 7.5 MeV (this addresses significant sparseness in the highest energy HEEF channel data).

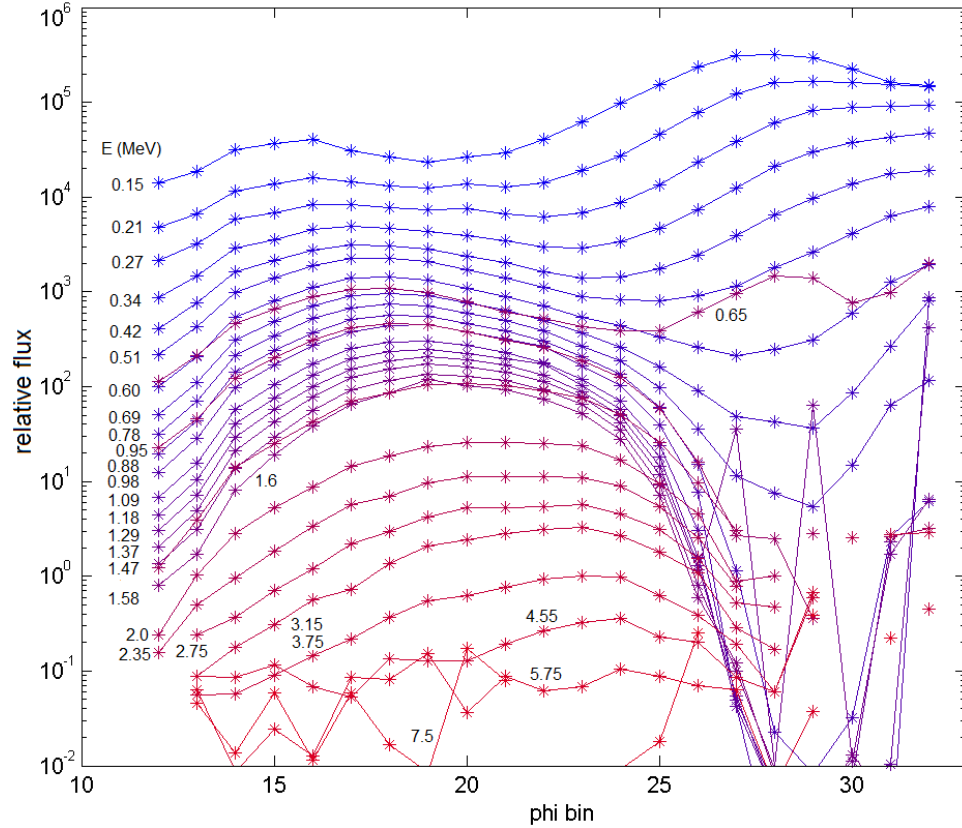


**Figure 21. Relative flux vs.  $\Phi$  bin for various CRRES MEA and HEEF channel energies.**

- 3) Smoothing of high energy channels,  $E \geq 3.75$  MeV (weighted average of neighboring bins in  $K$  and  $\Phi$ , addresses high variability in these channels resulting from low count statistics). Relative weighting of  $K$ -  $\Phi$  bins was [1 4 1; 4 10 4; 1 4 1] (i.e. nine bins were used with more weight on neighbors in  $K$  than in  $\Phi$ ).
- 4) Extrapolation of flux vs.  $\Phi$  curves to lower  $\Phi$  (=higher  $L^*$ ): the first ten  $K$  bins only and  $E < 1.5$  MeV only, obtain linear fit to (log flux) vs.  $L^*$ , require slope of each fit to be no greater than slope at next lowest energy, apply fit to lower  $\Phi$ , then smooth resulting curves (note: these results were largely over-written by the process described in Section 2.4.1.3).
- 5) Extrapolation of flux vs.  $K$  curves to higher  $K$ : obtain linear fit to log(flux) vs.  $K^{0.5}$ , constrain slope to  $-1 < m < -0.3$ , smooth slope values across  $\Phi$  slices, apply fit to higher  $K$  (note: these results were largely over-written by the process described in Section 2.4.1.3).
- 6) At each energy, identified isolated  $K$ - $\Phi$  bins with no data and filled these with the mean of immediate neighbor bins (three passes, but for poststorm templates one pass is done after high energy smoothing).
- 7) Interpolation of flux vs.  $E$  for each  $K$ - $\Phi$  bin for medium energies in the inner belt (data is sparse at  $L^* < 2.2$  or  $2.9$  pre/post-storm apart from HEEF 0.65 MeV and 0.95 MeV channels, so these are mostly used to set spectral shape for energies  $> 0.65$  MeV).
- 8) Smoothing at each energy (weighted average of neighboring bins in  $K$  and  $\Phi$ , same scheme as (3) above).

- 9) Apply spectral shape (flux vs.  $E$ ) for 2.35 MeV to higher energies in the inner belt ( $L^* < 2.2$  or 2.9 pre/post-storm).
- 10) Interpolate/extrapolate from CRRES energy channels to standard energy channels of AE9; these energies are:
  - AE9 standard energies: 0.04, 0.07, 0.10, 0.25, 0.50, 0.75, 1.00, 1.50, 2.00, 2.50, 3.00, 3.50, 4.00, 4.50, 5.00, 5.50, 6.00, 6.50, 7.00 MeV
  - MEA channel energies: 0.15, 0.21, 0.27, 0.34, 0.42, 0.51, 0.60, 0.69, 0.78, 0.88, 0.98, 1.09, 1.18, 1.29, 1.37, 1.47, 1.58 MeV
  - HEEF channel energies: 0.65\*, 0.95\*, 1.60\*, 2.00, 2.35, 2.75, 3.15, 3.75, 4.55, 5.75, 7.50 MeV (note that the three lowest energy HEEF channels were only used if no MEA data at comparable energies was available).
- 11) Smoothing at each energy in  $K$ - $\Phi$  space, using a relative weighting of [0 2 9 2 0; 5 15 34 15 5; 0 2 9 2 0] (i.e. eleven bins used, with more weight on neighbors in  $K$  than in  $\Phi$ ).

### 2.4.1.3 Production of template varieties

For each of the four basic templates from the process above, nine varieties were produced reflecting three choices for rate of flux decrease at low  $\Phi$  (high  $L^*$ ) and three choices for rate of flux decrease at high  $K$ . At low  $\Phi$ , flux vs.  $\Phi$  dependence was modeled as  $j \sim 10^{-a/\Phi}$  (after HEO-F3 observations at  $E=3$  MeV), with  $a=1.5, 1.7, \text{ or } 1.9$ . At high  $K$ , flux vs.  $K$  dependence was modeled as  $j \sim 10^{-K/b}$  (after TSX-5 CEASE observations), with  $b=2.5, 3, \text{ or } 3.5$ .

Some additional processing was applied to the results for use in AE9, including more smoothing and some adjustment of the inner belt fluxes. An example of the final templates is shown in Figure 22 as flux vs.  $\Phi$  and  $K$  for  $E=750$  keV.

### 2.4.1.4 Known issues

Several known issues with these templates exist. Representation at high  $L^*$ , high  $K$ , and high  $E$  is poorly constrained from CRRES data, hence the modeling and/or spectral shape duplications noted above. The inner electron belt data from CRRES is limited, mostly to lower HEEF energy channels in the pre-March 1991 storm period. Consequently these templates show insufficient variation with energy in the inner belt and slot region. (These issues in the inner belt are the primary reason that the CRRES templates were not used in V1.1.)

## 2.4.2 Summary

The above steps yielded 36 templates of log flux vs. energy,  $K$ , and  $\Phi$ , used in AE9 for processing data sets into flux maps, from four CRRES-derived base templates, each with three choices of extrapolation to low  $\Phi$  values and three choices of extrapolation to high  $K$  values.

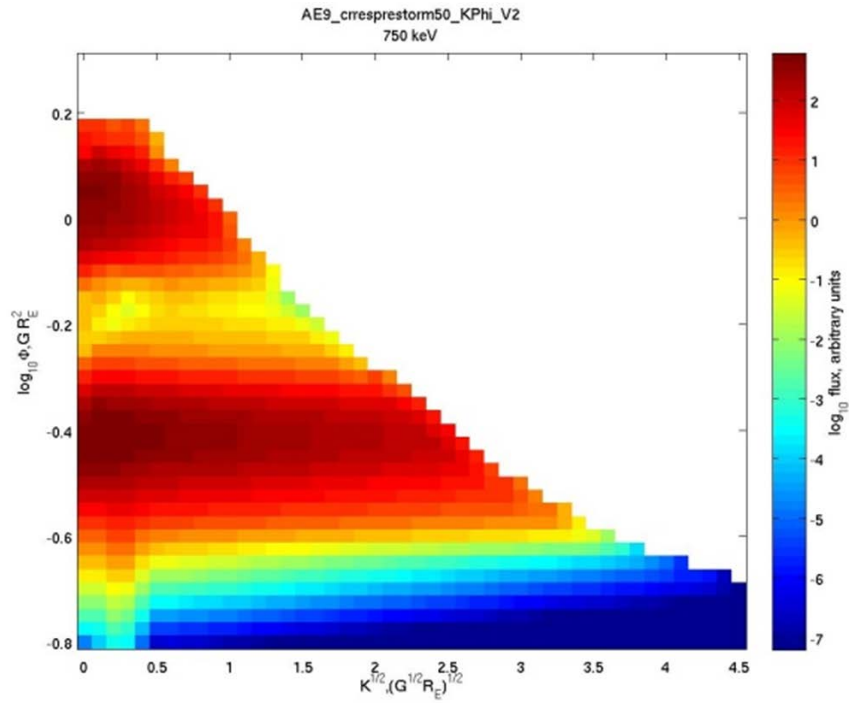


Figure 22. Illustration of final template results: CRRES prestorm,  $E=750$  keV.